University of Baghdad
College of Engineering
JE
JOURNAL OF ENGINEERING

Journal of Engineering

journal homepage: www.joe.uobaghdad.edu.iq

Volume 29 Number 3 March 2023

Directive and Steerable Radiation Pattern using SASPA Array

Rabah Abduljabbar Jasem
Ph.D.
Dept. of Electrical Engr.
Technical Institute of Al-Dour
Northern Technical Univ.
E-mail: rabah.aj@ntu.edu.iq
rabah_alobaidi5@yahoo.com

ABSTRACT

This work examines the ability of a special type of smart antenna array known as Switched Active Switched Parasitic Antenna (SASPA) to produce a directive and electronically steerable radiation pattern. The SASPA array consists of antenna elements that are switchable between active and parasitic states by using P-Intrinsic-N (PIN) diodes. The active element is the element that is supplied by the radio frequency while short-circuiting the terminals of an element in the array results in a parasitic element. Due to the strong mutual coupling between the elements, a directional radiation pattern with high gain and a small beamwidth can be produced with only one active element operating at a time. By changing the parasitic state to the active state sequentially for all elements, the directed radiation pattern can be easily rotated. The antenna array structure used in this work is the uniform circular array (UCA) to achieve symmetrical radiation patterns and full coverage of the entire azimuth plane. Also, a novel method for reducing the mutual coupling effect in SASPA arrays is proposed in this work. By using this method, some parameters of the generated SASPA's radiation pattern can be controlled. The simulated results obtained from this work depict that an *N*-element SASPA-UCA produces *N*-symmetrical, switchable, and steerable radiation patterns with high gain, small beamwidth, and a high Front-to-Back (F/B) ratio. Also, the results show that further improvements in these parameters can be achieved by increasing the number of elements in the array. Additional simulations demonstrate that by including decaying function weight in each element's circuitry, the mutual coupling between the components of the SASPA-UCA array can be minimized. The aforementioned parameters can then be efficiently modified using this mutual coupling reduction.

Keywords: beamwidth, F/B ratio, mutual coupling, smart antenna array, SASPA-UCA array.

*Corresponding author
Peer review under the responsibility of University of Baghdad.
https://doi.org/10.31026/j.eng.2023.03.01

Article received: 30/10/2022
Article accepted: 09/02/2023
Article published: 01/03/2023

نمط اشعاعي موجه وقابل للتوجيه باستخدام مصفوفة الهوائيات المتحولة بين حالتي الفعالة والطفيلية

رباح عبد الجبار جاسم
دكتوراه
الهندسة الكهربائية– المعهد التقني في الدور
الجامعة التقنية الشمالية

الخلاصة

تم في هذا العمل دراسة امكانية الحصول على نمط اشعاعي موجه وقابل للتوجيه الكترونيا الى اتجاهات مختلفة باستخدام مصفوفة تحتوي على هوائيات تتغير بين حالتين: الفعالة والطفيلية. الهوائي الفعال هو الذي يغذى بمصدر التردد الراديوي اما الهوائي الطفيلي هو الذي تكون اطراف تغذيته دائرة قصر. بوجود هوائي فعال واحد وبقية الهوائيات في حالة الطفيلية سيتم تكون نمط اشعاعي وبكسب عالي موجه الى اتجاه معين وعندما تكرر عملية التحول من طفيلي الى فعال لكل عنصر وعلى التوالي سيتم توجيه النمط الاشعاعي الى اتجاهات مختلفة وبسهولة. الاقتران المتبادل بين الهوائيات للطاقة المرسلة من الهوائيات نفسها تلعب دور اساسي في تكوين وتوجيه النمط الاشعاعي في هذه المصفوفات. كذلك سيتم دراسة امكانية تقليل خاصية الاقتران المتبادل هذه بطريقة جديدة. النتائج المستحصلة من هذا البحث تبين بان هذه المصفوفة لها القابلية على تكوين انماط شعاعية متماثلة وبعدد يساوي عدد عناصر المصفوفة وبكسب عالي وبعرض حزمة ضيقة و قيمة عالية لنسبة الاشعاع الامامي الى الخلفي. وكذلك فان النتائج تبين ان هذه العوامل من الممكن تحسينها عند زيادة عدد عناصر المصفوفة. نتائج اخرى في هذا العمل تبين من الممكن تغيير العوامل اعلاه باستخدام الطريقة المقترحة في هذا البحث حول تقليل ممانعة التبادل بين عناصر المصفوفة.

الكلمات الرئيسية: الهوائيات الذكية, الاقتران المتبادل , مصفوفات لهوائيات متحولة بين فعالة وطفيلية, عرض الحزمة

1. INTRODUCTION

Providing a radiation pattern with a directive, switched, rotatable, and small beamwidth main lobe is compulsory in wireless communication and mobile communication. This can be accomplished by making use of some of the key characteristics of smart antenna arrays, such as high gain, flexibility in producing beamformed main lobes on demand, simple hardware for supplying and changing the state of array elements, etc. Using these special antenna arrays will increase system efficiency, data throughput, user channels, connecting distance range, and reduce interference and Bit Error Rate (BER), e.g., as in Multiple-Input-Multiple-Output (MIMO) networks **(Omer et al., 2020)**. Also, smart antenna arrays can be used effectively for frequency location on demand due to their flexible characteristics **(Thiel and Smith, 2002; Lakshmi and Sivvam, 2017)**. As a result, the increased demand for modern services and facilities recently required in wireless communication systems can be accommodated **(Oluwole and Srivastava, 2018; Hamza and Al-Hindawi, 2021).**

One of these smart antenna arrays is the Switched Active Switched Parasitic Antenna (SASPA) array. In these arrays, each antenna is easily switched between active and parasitic states by simple electronic circuits involving PIN diodes **(Thiel and Smith, 2002).** The active element is

launched by the radio frequency supply, while the parasitic state is obtained when the terminals of the array element are short-circuited. The mutual coupling between the elements of SASPA arrays plays an important role in determining the resultant radiation pattern of these arrays. The main advantages of SASPA arrays are their inherent capability to accumulate radiated power in one direction at the expense of other directions, as well as their ability to steer their radiation pattern in a flexible manner **(Thiel and Smith, 2002; Wennestrom and Svantesson, 2001).** Additionally, compared to phased antenna arrays, the hardware needed to fabricate switched parasitic antenna arrays is more compact and occupies less space **(Islam et al., 2012)**. SASPA arrays are therefore valuable in equipment made into very small sizes. Therefore, the abovementioned features of switched parasitic antenna arrays might be efficient for the demands of current 5G networks and the Internet-of-Things (IoT) **(Kausar et al., 2016)**. In **(Thiel and Smith, 2002),** SASPA arrays have been proposed and studied as effective and versatile antenna arrays for cellular communications. However, the mutual coupling between the elements in SASPA arrays has not been extensively studied, although this unavoidable phenomenon is an important factor in examining the performance of SASPA arrays.

The characteristics of the SASPA structured as a uniform circular array, i.e., SASPA-UCA, are investigated in this work as those of a smart antenna array capable of producing symmetrical radiation patterns with a narrow main beam, high gain, a small back lobe, almost no side lobes, and the ability to cover the entire azimuthal plane. Additionally, a proposed method for managing these parameters by reducing the mutual coupling phenomenon between the SASPA array's elements will be investigated.

2. THE STRUCTURE OF THE SASPA ARRAY

A SASPA-UCA consisting of *N* half-wave dipole antenna elements is shown in **Fig. 1**. The array is placed in the *x-y* plane, with its center at the origin. The dipoles are vertically oriented, parallel to the *z-axis*, and equally spaced along the perimeter of a circle of radius *R*. The interelement spacing between the elements is *d* in wavelengths. The radius *a* of each dipole is supposed to be very small compared to the wavelength of the launched radio signal, i.e., $a \ll \lambda$, accordingly, the current flowing in each element will have sine wave distribution **(Balanis, 2016)** with zero current at the ends of the element (Kishore, 2009). As a result, the maximum radiation for each element will be in the *x-y* plane ($z = 0$ plane) if the element is derived at its centre.

All the elements in the SASPA-UCA are parasites at the same time, but one element is active. The resultant radiation pattern in the azimuth plane will be directed in the direction of and away from the active element. This occurs because the parasites act as reflectors for the radiated energy behind the active element. Accordingly, a directive main beam with a small beam width will be obtained. The next time, a new element is changed to the active state while the first active element is switched back to the parasitic state. As a result, the main beam is now rotated in the direction of and away from the new active element. The same procedure is repeated for all elements sequentially, and a symmetrically steered beam that covers the azimuth plane will be achieved **(Thiel and Smith, 2002)**. The switching between active and parasitic states can be easily accomplished using PIN diodes. These diodes are commonly used in microwave circuits because of their very short switching times, very low resistance in forward bias conditions, and very high resistance in reverse bias conditions.

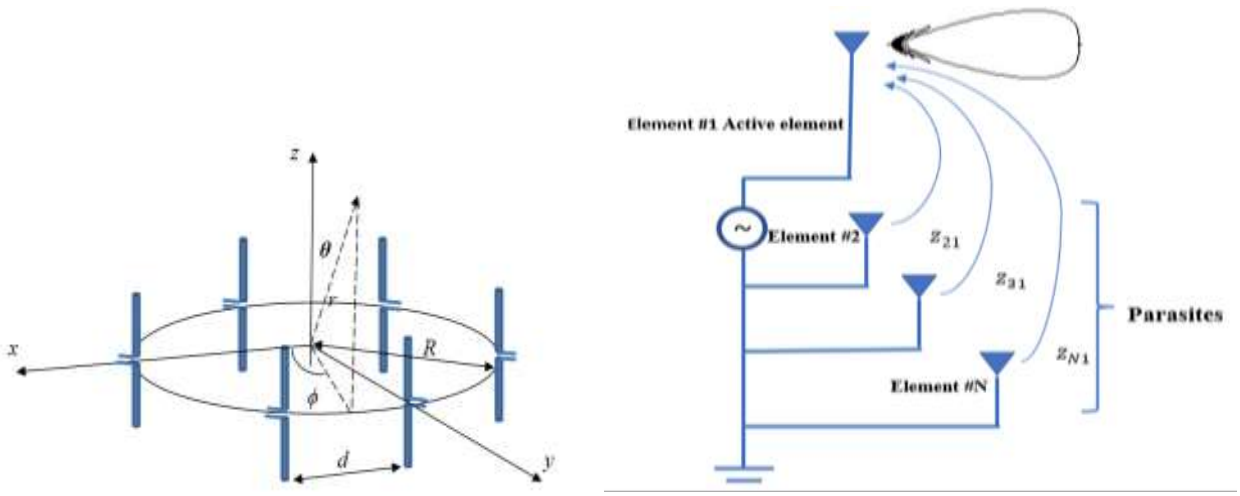

(a) (b)

Figure 1. A SASPA-UCA consists of half-wave dipole antennas. (a) the structure, (b) the mechanism of coupling the parasites to the active element through mutual coupling.

3. THE RADIATION FIELD OF SASPA-UCA

The total electric far field of an array made up of two half-wave dipole antennas placed side by side, with one of them operating as an active element and the other as a parasitic element, is described in **(Thiel and Smith, 2002)** as follows:

$$E_t(\mathrm{r},\theta,\phi) = \frac{j\omega\mu}{2\pi kr}\frac{\cos\left(\frac{\pi}{2}cos\theta\right)}{sin\theta}\left(i_c + i_p e^{-jkdcos\phi}\right) \quad (1)$$

where, r,θ,ϕ are the spherical coordinates. The currents i_c , i_p are respectively active and parasitic currents. ω is the radian frequency of the supply, μ is the permeability, r is the radial distance to the observation point, and k is the wave number. Eq. (1) can be rewritten in vector form as:

$$E_t(\mathrm{r},\theta,\phi) = \gamma(\theta) i^T a(\phi) \quad (2)$$

where, $i = \left(i_c * i_p\right)^T$, $a(\phi) = \left(1 * e^{-jkdcos\phi}\right)^T$ are column vectors, and $(.)^T$ is the transpose operation. In this work, the bold lowercase letter refers to a vector, and the bold uppercase letter refers to a matrix. The factor $\gamma(\theta) = \frac{j\omega\mu}{2\pi kr}\frac{\cos\left(\frac{\pi}{2}cos\theta\right)}{sin\theta} = \frac{j\omega\mu}{2\pi kr} = \gamma =$ constant, if only the azimuthal component of the radiated electric field is considered, i.e., when $\theta = \pi/2$ and observed at a fixed distance. This gives only ϕ dependency for the radiated electric field in Eq. (2). Note that the currents in Eq. (1) are the complex values (amplitude and phase) of the coupled currents. $a(\phi)$ is known in the literature as the steering vector **(Krim and Viberg, 1996)**. Eq. (2) can be updated for the case of N-element SASPA-UCA shown in **Fig. 1** as:

$$E_t(\phi) = \gamma i^T a_{UCA}(\phi)$$
$$= \gamma\left(i_{p_1} \;\; i_{p_2} \ldots i_c \ldots \; i_{p_{N-1}}\right)^T \left(e^{-jkR\cos\phi} \quad e^{-jkR\cos\left(\phi - \frac{2\pi}{N}\right)} \ldots e^{-jkR\cos\left(\phi - \frac{2\pi(N-1)}{N}\right)}\right) \qquad (3)$$

Where $i \in \mathbb{C}^{N\times 1}$ is the coupled current vector, and $a_{UCA}(\phi)\mathbb{C}^{N\times 1}$ is the steering vector of the UCA **(Krim and Viberg, 1996)**. The current vector i in Eq. (3) can be related to the supply voltage, v_c that supplies the active element *c* through the relationship:

$$v = Zi \qquad (4)$$

where, $v = (0 \;\; 0 \;\; v_c \;\; 0 \;\; \ldots .0)^T$, is the vector of supply voltages with all zero entries except v_c . $Z \in \mathbb{C}^{N\times N}$ is the mutual coupling matrix defined as:

$$Z = \begin{bmatrix} Z_{11} & Z_{12} \ldots Z_{13} & Z_{12} \\ Z_{12} & Z_{11} \ldots . Z_{12} & Z_{13} \\ \vdots & \vdots & \\ Z_{12} & Z_{13} \ldots . Z_{12} & Z_{11} \end{bmatrix} \qquad (5)$$

where, Z_{rr} is the self-impedance of the antenna element *r* and Z_{rs} is the mutual impedance between antenna elements *r* and *s*. The formulae for these impedances can be found in **(Balanis, 2016)**, in which the principle of the induced EMF method is used to derive the formulae for self and mutual impedances for two dipole antennas placed in a side-by-side configuration. Notice that the matrix *Z* is circulant Toeplitz in the case of UCA since $Z_{rr} = Z_{ss}$, $Z_{rs} = Z_{sr}$, and each column (row) is the cyclic permutation of the previous column (row) **(Gray, 2006)**. The complex values of Z_{rs} are mainly determined by the distance between the elements. Plugging Eq. (4) into Eq. (3) yields:

$$E_t(\phi) = \gamma v^T (Z^{-1})^T a_{UCA}(\phi) \qquad (6)$$

4. REDUCTION IN MUTUAL COUPLING

The mutual coupling phenomenon is generally considered an adverse effect in all-active antenna arrays **(Singh et al., 2013)**. When these arrays are used as direction finders, for example, the measurements contaminated by the effect of mutual coupling result in inaccurate estimates of DOAs **(Chen and Kiang, 2014; Yeh et al., 1989)**. Many methods have been proposed in the literature for eliminating the effect of mutual coupling such as by **(Saenz, et al., 2009; Sun and Cao, 2017)** and others.

However, mutual coupling is the key characteristic of SASPA arrays. It is obvious from Eq. (6) that the mutual coupling significantly determines the shape and the direction of the resultant radiation pattern of SASPA arrays. Thus, by controlling the effect of this unavoidable phenomenon, some important parameters of the radiation patterns of SASPA, such as gain, beamwidth, and front-to-back ratio, can be governed. It is well-known in the literature that the variation of the real component or the imaginary component of the mutual coupling impedance Z_{rs} between two dipole antennas *r* and *s* placed in a side-by-side configuration mainly depends on the spacing between them. It is evaluated as:

$$Z_{rs} = R_{rs} \pm jX_{rs} \tag{7}$$

Fig. 2 shows these variations which are derived from the principle of the induced EMF concept **(Balanis, 2016)**.

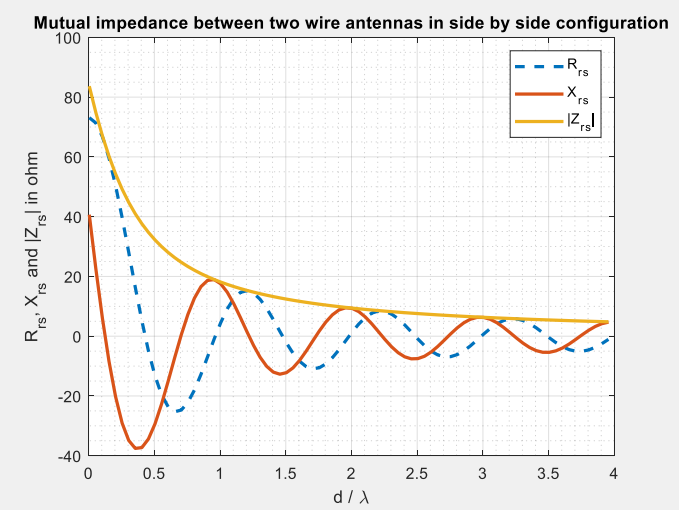

Figure 2. The mutual coupling impedance Z_{rs} as a function of the distance in wavelength between two dipole antennas structured in a side-by-side configuration.

It can be seen from **Fig. 2** that the magnitude of the mutual coupling impedance, i.e., $|Z_{rs}(d)|$ in Ω, is inversely proportional to the interelement spacing. This proportionality is almost a decaying function. Thus, the mutual coupling between far-distant elements almost vanishes in an antenna array. If it is required that the mutual coupling between the close elements be reduced, a further decay to the envelope of **Fig. 2**, i.e., $|Z_{rs}(d)|$, can be applied. To achieve this, an exponentially decaying function can be used. Thus, multiplying $|Z_{rs}(d)|$ by another exponentially decaying function results in more reduction in the influence of the mutual coupling between the elements of the array.

The function $e^{-d/x}$, where x (in wavelengths) is called the distance constant, can be used to reduce the effect of the mutual coupling between antenna array elements, as shown by the plot of **Fig. 3a**. The appropriate value of x can be found so that at a chosen distance on the array away from a certain element (usually the reference element), $|Z_{rs}(d)|$ almost vanishes. $|Z_{rs}(d)|$ could be approximated by the function $h(d)$ as:

$$|Z_{rs}(d)| \approx h(d) = Ae^{-d^{\alpha}/y} + B \qquad \Omega \tag{8}$$

where α and y (in wavelengths) can be determined empirically, $A = |Z_{rs}(0)| - B$ and B is the steady state of $h(d)$ when $d^{\alpha} \gg y$. It is commonly assumed that for an exponentially decaying function, its steady state occurs when $d^{\alpha} \geq 5y$. In this work, it is assumed that the maximum distance between the reference element and the farthest element in the array is $d_{max}/\lambda = 3$ since the SASPA array is usually structured in a very small aperture. For $\alpha = 0.75$, and $y = 0.6$, $h(d)$ may be expressed as:

$$h(d) = 80.66e^{-\frac{d^{0.75}}{0.6}} + 3 \qquad 0 \le d_{max} \le 3\lambda \tag{9}$$

Fig. 3a shows the approximated function $h(d)$ along with $|Z_{rs}(d)|$. When $|Z_{rs}(d)|$ is multiplied by $e^{-d/x}$, the resultant new magnitude of the mutual impedance function will have the mathematical expression:

$$|Z_{rs}(d)|e^{-d/x} \approx Aexp\left(-\frac{xd^{\alpha}+yd}{yx}\right) + Bexp\left(\frac{-d}{x}\right) \tag{10}$$

The value *x* can be mainly determined from the first term of the RHS of Eq. (10) since $B \ll A$. By setting the exponent of this term to the value one where 37% of $|Z_{rs}(0)|$ is obtained, the range of *x* can be calculated to have an efficient reduction in the mutual coupling impedance and to choose the vanishing point for this impedance, which is at approximately $xd^{\alpha} + yd = 5xy$. Thus, the value of *x* can be determined from $x = \frac{yd}{y-d^{\alpha}}$ for given y and α. Note that the range of *x* should be $0 < x \le 1$ so that the decay condition for $e^{-d/x}$ is satisfied. **Fig. 3b** shows the variation of *x* versus *d*. It can be seen from this figure that the useful range for *d* to have the above range of x is $0 < d < 0.4$. **Fig. 3a** shows the reduced mutual impedance, i.e., $|Z_{rs}(d)|e^{-d/x}$ and the reduced $h(d)$ i.e., $h(d)e^{-d/x}$ when $x = 0.5\lambda$. In **Fig. 3c**, it is shown that a significant reduction in the mutual coupling components has been achieved when multiplying $|Z_{rs}(d)|$ by the function the $(e^{-d/0.5})$.

5. WEIGHTED SASPA ARRAY

The method explained in the previous section can be applied to SASPA arrays to decrease the effect of the mutual coupling between the elements of the array. The result is reshaping the radiation patterns with changed parameters, such as the front-to-back (F/B) ratio and beam width. Also, the nulls in the radiation pattern can be eliminated. Furthermore, reducing the mutual coupling results in reducing the overall gain of the SASPA array. This can be obtained by multiplying the entries of the weight vector:

$$w = \left[1 \;\; e^{-d/x} \;\; e^{-2d/x} \ldots \; e^{-(N-1)d/x}\right] \tag{11}$$

by the corresponding elements of the SASPA array with the active element weighting one as shown in **Fig. 4.** When the array is SASPA-UCA, the weight vector in Eq. (11) should accommodate the positional or structural symmetry between the elements. Thus, the weight matrix *W* should have the following circulant Toeplitz structure:

$$W = \begin{bmatrix} 1 & e^{-d/x} \ldots e^{-2d/x} & e^{-d/x} \\ e^{-d/x} & 1 \ldots . e^{-d/x} & e^{-2d/x} \\ \vdots & \vdots & \\ e^{-d/x} & e^{-2d/x} \ldots . e^{-d/x} & 1 \end{bmatrix} \tag{12}$$

and Eq. (6) for weighted SASPA-UCA becomes:

$$E_t(\phi) = \gamma v^T (W \odot Z^{-1})^T a_{UCA}(\phi) \quad (13)$$

where, $\odot$ denotes the Hadamard product operation **(Horn and Johnson, 2013).**

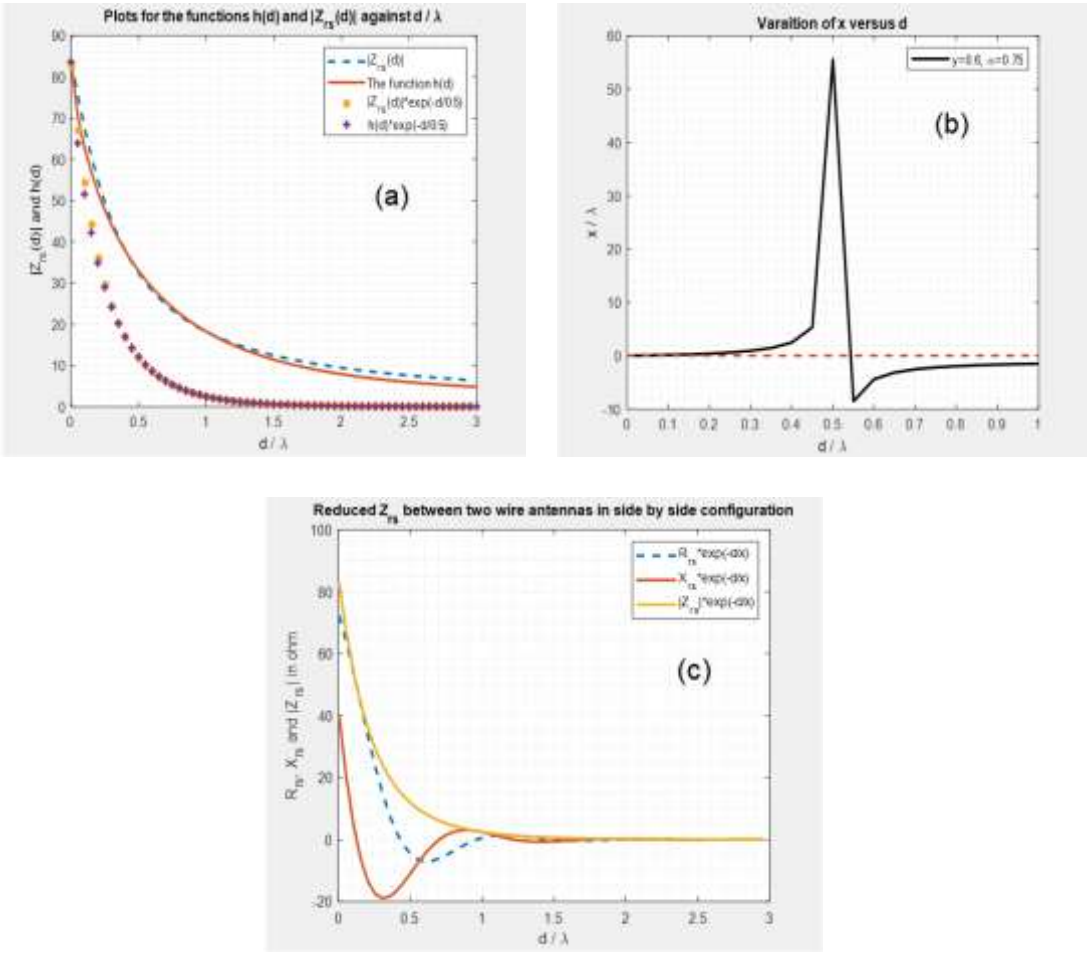

Figure 3. (a) Plots for $|Z_{rs}(d)|$and the approximated function $h(d)$ against d, (b) Variation of x versus d (c) reduced mutual coupling impedance.

6. SIMULATION RESULTS AND DISCUSSION

In this section, several simulations will be conducted to show how a SASPA-UCA produces a directive radiation pattern and how this pattern can be electronically steered and covers the entire azimuth plane. This facility can be achieved when one element at a time in an *N*-element SASPA-UCA is switched to the active state while keeping the other elements as parasites. Also, controlling some parameters of antenna arrays as a consequence of lowering the effect of the mutual coupling phenomenon is illustrated in these simulations.

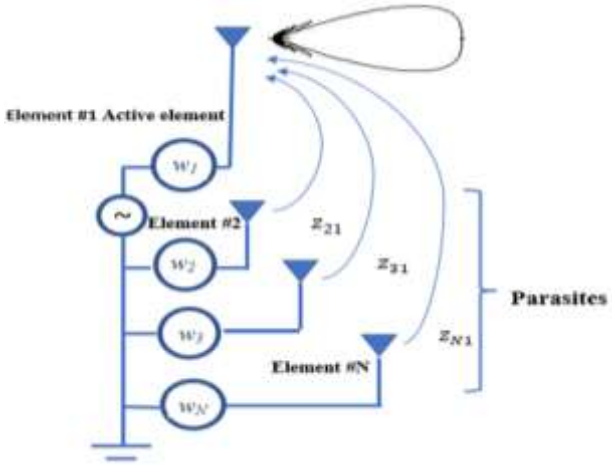

Figure 4. Weighted SASPA array.

Firstly, an array consisting of four half-wave dipoles is used in a structure similar to the one shown in **Fig. 1**. The radius of the array is $R = 0.1\lambda$. **Fig. 5** shows the resultant electric far fields (horizontal plane or azimuth plane) in dB in the *x*-*y* plane, which are generated according to Eq. (6) when one element is active at a time and the others are parasites. It can be seen that the resulting radiation patterns due to successively converting each element to an active state at one time are symmetrical, with the maximum value of the main lobe (the gain) being directed at the angles $\phi = ((n-1)/N) \times 360^{\circ}$ $n = 1,2,3,4$. **Fig. 6** depicts that increasing the number of antenna elements from four to six results in increasing the number of switched radiation patterns and decreasing the area of sectors that are covered by the radiation patterns of the previous array. Also, the gain of the main lobe in the six-element SASPA-UCA is greater than the gain of the main lobe in the four-element SASPA-UCA, as depicted in **Table 1.** Moreover, the Front-to-Back (F/B) ratio for the six-element SASPA-UCA is significantly increased. In addition, a narrower beamwidth BW (in degrees) is obtained when N=6 as compared with 4-element SASPA-UCA. This proves that better directivity can be obtained when increasing the number of elements in the array.

The values calculated and listed in **Table 1** also demonstrate that the parameters, gain, F/B ratio, and beamwidth can be changed by using weights that are inserted into the circuitry of the elements of SASPA-UCA. Each weight of the matrix W in Eq. (12) is multiplied by the corresponding mutual impedance Z_{rs} and a reduction in mutual coupling is obtained. Two values of the distance constant, $x = 0.5\lambda$, and $x = 0.25\lambda$ are used. As a result, the array gain has been noticeably decreased and the BW widens when compared with the unweighted SASPA-UCA. However, the F/B ratio increased when $x = 0.5\lambda$ and then decreased when $x = 0.25\lambda$ for both values of N. The reason is that the value of this ratio depends on the strength of either the main lobe or the back lobe, whichever dominates (the energy coupled from each parasitic element into the active element may be constructive or destructive, depending mainly on the distance between the elements). **Figs. 7 and 8** confirm the above results, in which the radiation patterns for SASPA-UCA and weighted SASPA-UCA are compared.

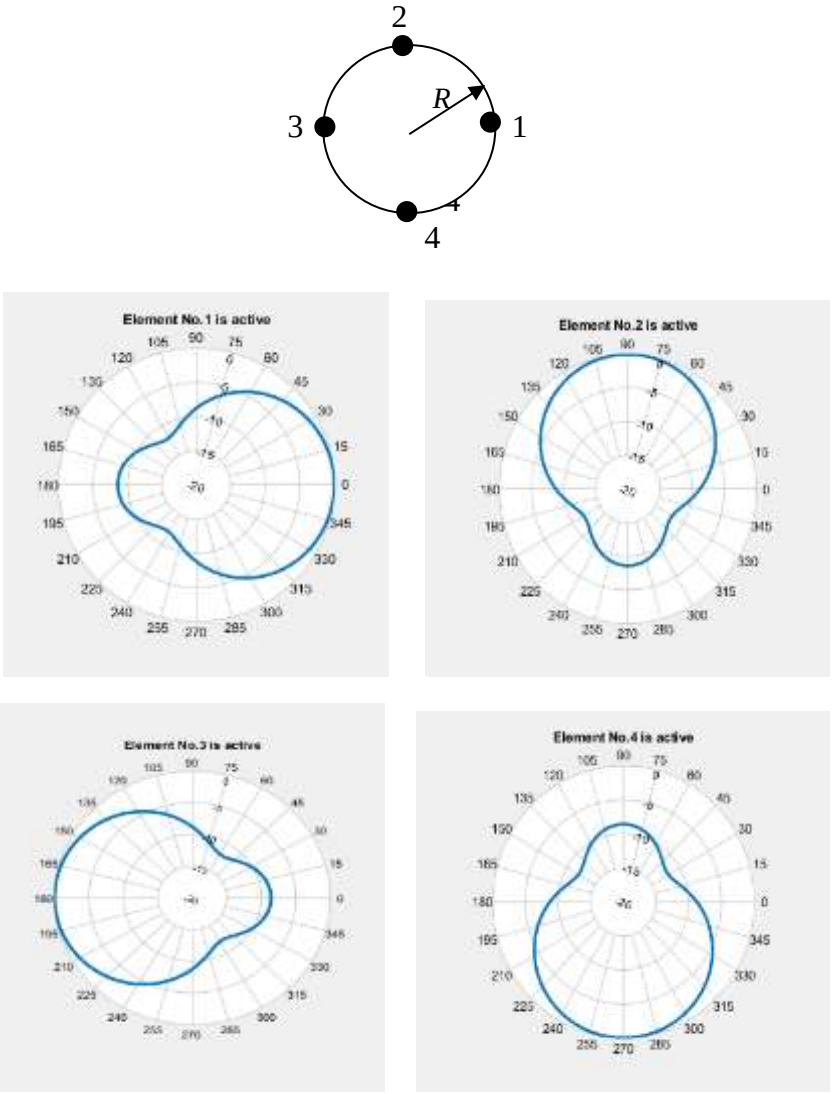

Figure 5. Normalized E-field (horizontal plane) radiation patterns of a four element SASPA-UCA. The elements are half-wave dipoles. The radius of the array is $R = 0.1\ \lambda$.

Table 1. A comparison between some parameters of SASPA-UCA and weighted SASPA-UCA arrays. The radius of the array is $R = 0.1\lambda$.

Array	No. of elements	Array parameters		
		$(G)_{dB}$	$(F/B)_{dB}$	$(BW)^{o}$
SASPA-UCA	4	12.52	8.59	100
	6	19.97	9	96
Weighted SASPA-UCA x = 0.5λ	4	10.15	9.14	108
	6	19.1	10.85	106
Weighted SASPA-UCA x = 0.25λ	4	7.49	7.18	128
	6	8.93	8.56	134

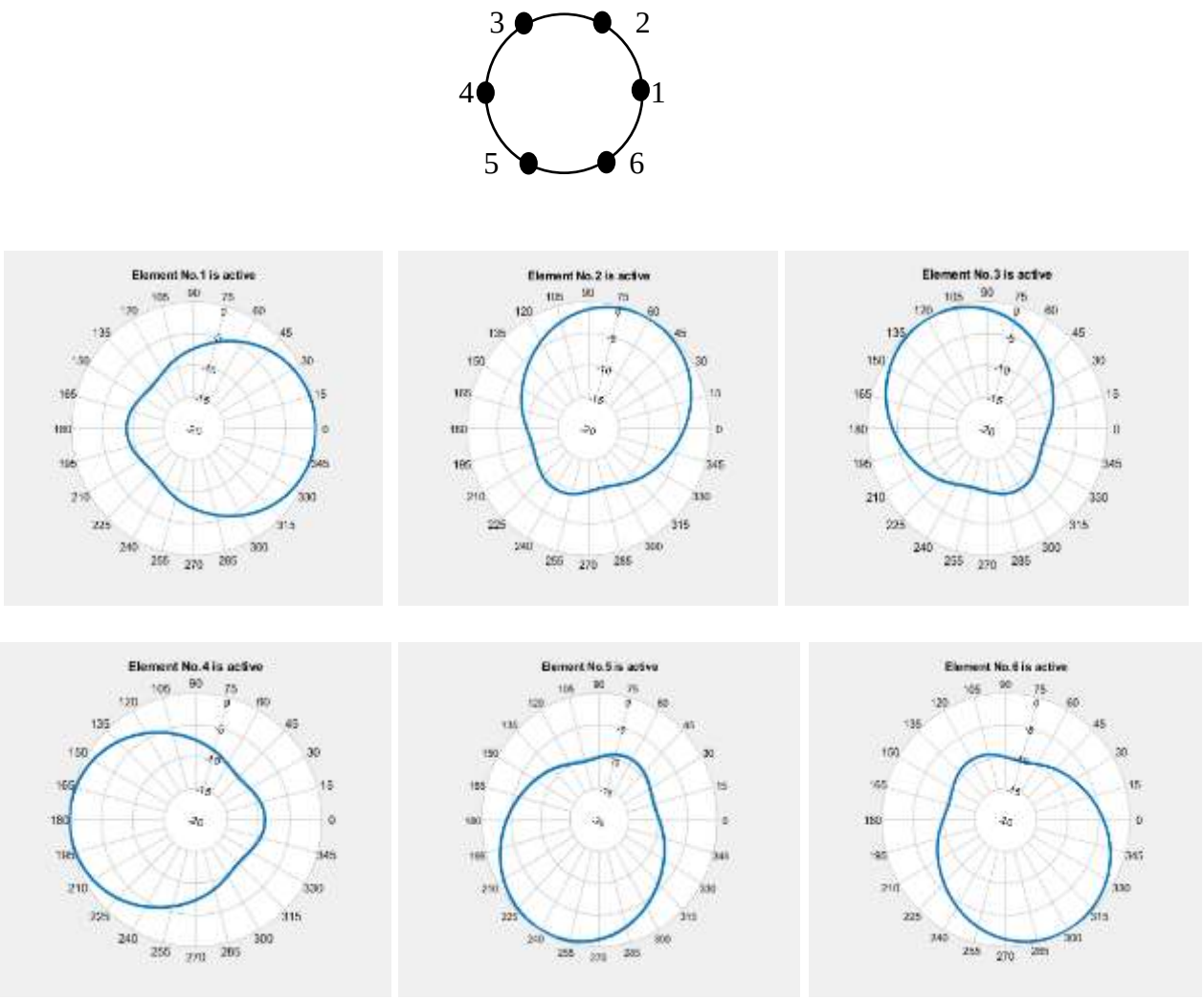

Figure 6. Normalized E-field (horizontal plane) radiation patterns of a six-element SASPA-UCA. The elements are half-wave dipoles.
The radius of the array is $R = 0.1\ \lambda$.

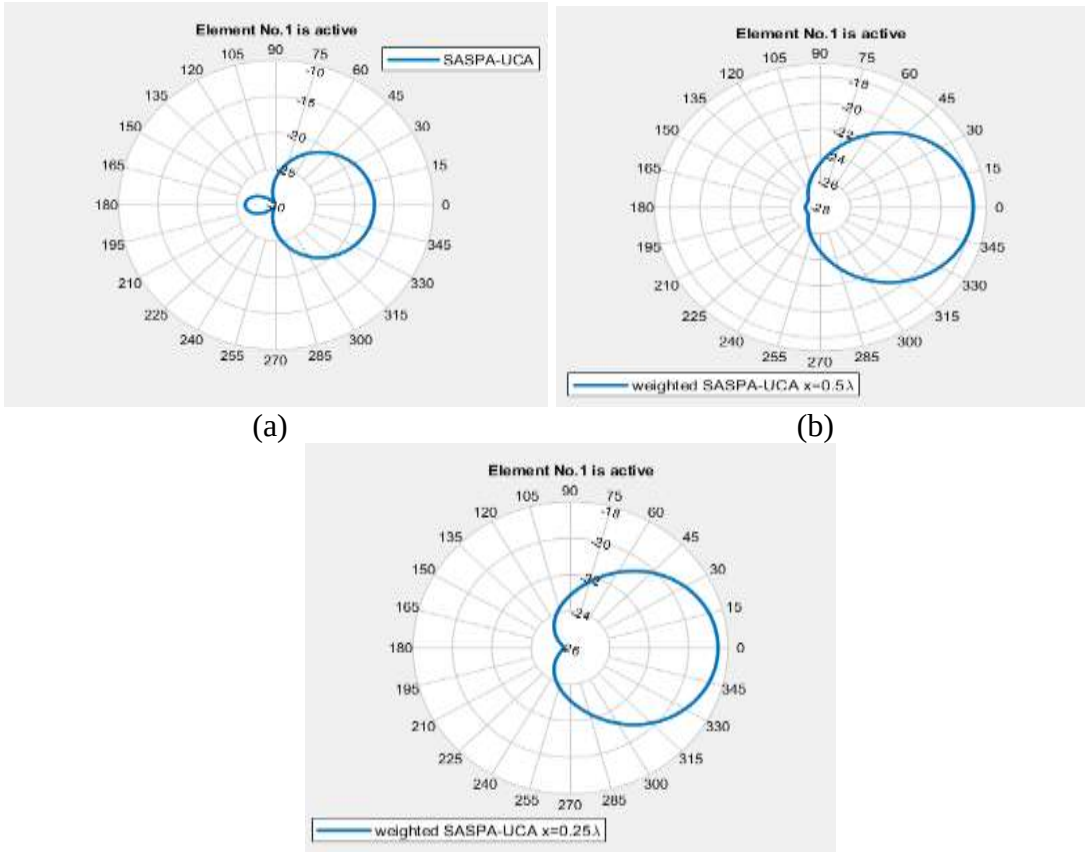

Figure 7. Comparison between E-field radiation patterns of SASPA-UCA and weighted SASPA-UCA arrays. $N = 4$, $R = 0.1\ \lambda$. (a) without mutual coupling reduction, (b) with mutual coupling reduction using $x = 0.5\ \lambda$, (c) with mutual coupling reduction using $x = 0.25\ \lambda$. Element *No. 1* is active in all cases.

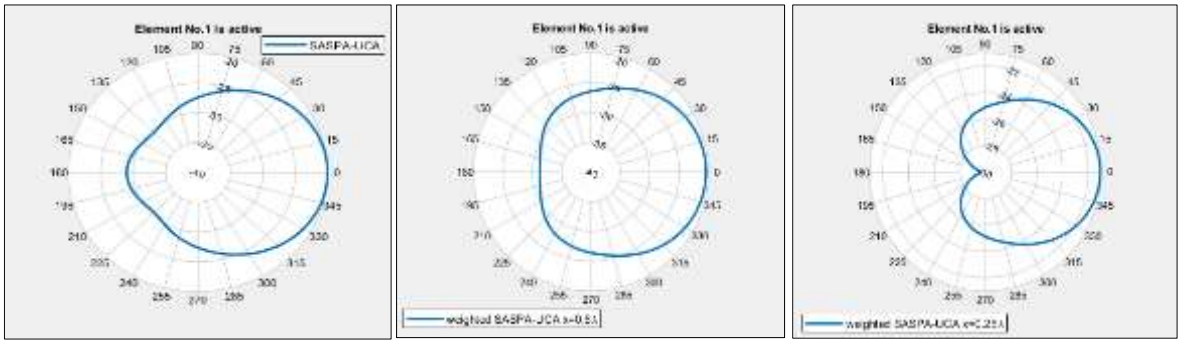

Figure 8. Comparison between E-field radiation patterns of SASPA-UCA and weighted SASPA-UCA arrays. $N = 6$, $R = 0.1\ \lambda$, (a) without mutual coupling reduction b) with mutual coupling reduction using $x = 0.5\ \lambda$, (c) with mutual coupling reduction using $x = 0.25\ \lambda$. Element *No. 1* is active in all cases.

7. CONCLUSIONS

The performance of a Switched Active Switched Parasitic-Uniform Circular Antenna array (SASPA-UCA) in terms of some parameters have been studied in this work. The outcomes of this work can be concluded as:

- Using the SASPA-UCA, a directive radiation pattern with high gain, a high F/B ratio, and a small beamwidth of the main lobe can be achieved.
- By successively switching each element in the array from the parasitic state to the active state, the directive SASPA-UCA's radiation pattern may be easily rotated to span the whole azimuth plane.
- Increasing the number of elements in the array results in enhancing the abovementioned parameters.
- The features of the SASPA-UCA are inherently available and easily accessible in these arrays due to the strong mutual coupling phenomenon between the elements of the array. Thus, by reducing this phenomenon, the array parameters can be controlled. It is depicted that by using weights with a decaying function along with the elements in SASPA-UCA, the effect of the mutual coupling can be significantly reduced.
- Working out the proposed method in the last item, the useful range for the decaying factor has been specified to have an effective reduction in mutual coupling. Accordingly, the gain, F/B ratio, and beamwidth can be varied.

In conclusion, SASPA-UCA can be considered smart antenna arrays that are beneficial for wireless communication since these arrays provide key characteristics that are valuable, flexible, and controllable and can be installed in compact-sized instruments.

REFERENCES

Balanis, C. A., 2016. *Antenna Theory: Analysis and Design.* 4th ed., John Wiley and Sons.

Chen,, K. H., and Kiang, J. F., 2014. Mutual Coupling Componsation in Direction of Arrival Estimation with a Linear Dipole Array. *2014 USNC-URSI Radio Science Meeting (Joint with AP-S Symposium),* pp. 116-116, doi: 10.1109/USNC-URSI.2014.6955498.

Gray, R. M., 2006. *Toeplitz and Circulant Matrices: A Review.* now Publisher Inc.

Hamza, A. R., and Al-Hindawi, A. M. J., 2021. The Effecting of Human Body on Slotted Monopole Antenna in Wearable Communications. *Journal of Engineering*, 27(2), pp. 27-43. doi: 10.31026/j.eng.2021.02.03.

Horn, R. A., and Johnson, C. R., 2013. *Matrix Analysis.* 2nd ed., Cambridge University Press, New York, USA.

Islam, M. R., Chamok, N. H., and Ali, M., 2012. Switched Parasitic Dipole Antenna Array for High-Data-Rate Body-Worn Wireless Applications. *IEEE Antennas and Wireless Propagation Letters,* 11, pp. 693-696. doi: 10.1109/LAWP.2012.2204949.

Lakshmi, T.J., and Sivvam, S., 2017. Smart Antennas for wireless communication. *International Journal of Applied Engineering Research*, 12(1), p. 2017.

Kausar, A., Mehrpouyan, H., Sellathurai, M., Qian, R., and Kausar, S., 2016. Energy Efficient Switched Parasitic Array Antenna for 5G Networks and IoT. *Loughborough Antennas Propagation Conference (LAPAC).* doi: 10.1109/LAPC.2016.7807569.

Kishore, K., 2009. *Antenna and Wave Propagation.* I.K. International Publishing House Pvt. Ltd.

Krim, H., and Viberg, M., 1996. Two Decades of Array Signal Processing Approach. The Parametric Approach. *IEEE Signal Processing Magazine,* 13(4), pp. 67-94, doi: 10.1109/79.526899.

Oluwole, A. S., and Srivastava, V. M., 2018. Features and Futures of Smart Antennas for Wireless Communications: A Technical Review. *Journal of Science and Technology Review,* 11(4), pp. 8-24. doi:10.25103/jestr.114.02.

Omer, D. S., Hussien, M. A., and Mina, L. M., 2020. Ergodic Capacity for Evaluation of Mobile System Performance. *Journal of Engineering,* 26(10), pp. 135-148. doi: 10.31026/j.eng.2020.10.10.

Saenz, E., Ederra, I., Gonzalo, R., Pivnenko, S., Breinbjerg, O., and de Maagt, P., 2009. Coupling Reduction Between Dipole Antenna Elements by Using a Planar Meta-Surface. *IEEE Transactions on Antennas and Propagation,* 57, pp. 383-394. doi: 10.1109/TAP.2008.2011249.

Singh, H., Sneha, H. L., and Jha, R. M., 2013. Mutual Coupling in Phased Arrays: A Review. *International Journal of Antennas and Propogation,* ID 348123. doi:10.1155/2013/348123.

Sun, X., and Cao, M., 2017. Mutual Coupling Reduction in An Antenna Array by Using Two Parasitic Microstrips. *International Journal of Electronics and Communications,* AEU, 74, pp. 1-4. doi:10.1016/j.aeue.2017.01.013.

Thiel, D. V., and Smith, S., 2002. Switched Parasitic Antennas for Cellular Communications. Artech House.

Wennstrom, M., and Svantesson, T., 2001. An Antenna Solution for MIMO Channels: The Switched Parasitic Antenna*. 12th IEEE International Symposium on Personal, Indoor and Mobile Radio Communications*, pp. A159-A163. doi: 10.1109/PIMRC.2001.965412.

Yeh, C. C., Leou, M. L., and Ucci, D. R., 1989. Bearing Estimation with Mutual Coupling Present. *IEEE Transactions on Antennas and Propagation,* 37(10), pp. 1332-1335. doi: 10.1109/8.43546.